Analysis of Combined Conductive-Radiative Heat Transfer in a Two-Dimensional Rectangular Enclosure With a Gray Medium

W. W. Yuen

E. E. Takara

Department of Mechanical and Environmental Engineering,
University of California at Santa Barbara,
Santa Barbara, CA 93106

Combined conductive-radiative heat transfer in a two-dimensional enclosure is considered. The numerical procedure is based on a combination of two previous techniques that have been demonstrated to be successful for a two-dimensional pure radiation problem and a one-dimensional combined conductive-radiative heat transfer problem, respectively. Both temperature profile and heat transfer distributions are generated efficiently and accurately. Numerical data are presented to serve as benchmark solutions for two-dimensional combined conductive-radiative heat transfer. The accuracy of two commonly used approximation procedures for multidimensional combined conductive-radiative heat transfer is assessed. The additive solution, which is effective in generating approximation to one-dimensional combined conductive-radiative heat transfer, appears to be an acceptable empirical approach in estimating heat transfer in the present two-dimensional problem. The diffusion approximation, on the other hand, is shown to be generally inaccurate. For all optical thicknesses and conduction-radiation parameters considered (including the optically thick limit), the diffusion approximation is shown to yield significant errors in both the temperature and heat flux predictions.

1 Introduction

Combined conductive-radiative heat transfer in a multidimensional enclosure is a problem of considerable practical importance. Until now, most of the reported work in this area has been confined to either combined conduction-radiation in a one-dimensional planar system (Viskanta and Grosh, 1962; Einstein, 1963; Yuen and Wong, 1980) or pure radiation in multidimensional systems (Glatt and Olfe, 1973; Modest, 1975; Ratzel and Howell, 1982; Yeun and Wong, 1984). A series of recent works by Howell et al. (1982, 1984, 1985) appears to contain the only reported solutions in the literature that deal with the combined conductive-radiative heat transfer in a system with multidimensional geometry.

Fundamentally, the difficulty associated with multidimensional combined conductive-radiative heat transfer lies in its extreme mathematical complexity. The energy balance equation is a highly nonlinear partial differential integral equation. While exact analytical solutions are practically impossible to obtain, numerical solutions are difficult and time consuming. Numerical results presented by Razzaque et al. (1984), for example, are mainly those with moderate or large values of the conduction-radiation parameter ($N_1 \geq 0.05$). For cases with low values of the conduction-radiation parameter, the authors noted that "the method requires a substantial amount of computer time to achieve convergence."

In a recent series of works by Yuen et al. (1984a, 1984b, 1985), a numerical technique was developed for two-dimensional pure radiation problems. Utilizing tabulated values of a class of generalized exponential integral function, $S_{\bar{n}}(x)$, numerical results were generated accurately and efficiently (cpu time on an 11/780 Vax computer for a typical two-dimensional pure radiation calculation is less than 1 min). In another work on one-dimensional combined conductive-radiative heat transfer (Yuen and Wong, 1980), an iterative procedure, in which the blackbody emissive power is not required to satisfy the no-slip condition at the boundary, was shown to be effective in solving the highly nonlinear differential integral governing equation. The objective of the present work is to demonstrate that the same numerical technique and iteration procedure are also effective in analyzing two-dimensional combined conductive-radiative heat transfer problems. Based on numerical results, the general characteristics of two-dimensional combined conductive-radiative heat transfer are discussed.

It is important to note that due to the mathematical complexity associated with radiation, some approximate procedures are probably necessary for analysis of combined conductive-radiative heat transfer in practical engineering systems. Until now, development of such approximation methods has been difficult because of the lack of an available numerical "benchmark" solution. As is illustrated in the later sections, numerical results generated in the present work are accurate. In addition to illustrating the important physics of combined conductive-radiative heat transfer, these results can serve as a valuable basis for such development. Specifically, the additive solution, which has been shown to be quite accurate for one-dimensional combined conductive-radiative heat transfer (Einstein, 1963; Yuen and Wong, 1980), is demonstrated to be also an accurate empirical procedure to determine two-dimensional combined conductive-radiative heat transfer. The diffusion approximation, which is still one of the common techniques utilized by industries in estimating the effect of radiative heat transfer in practical engineering systems, is shown to be highly inaccurate for two-dimensional problems. For all optical thicknesses and conduction-radiation parameters considered, the diffusion approximation is shown to yield significant errors in both the temperature and heat flux predictions.

Contributed by the Heat Transfer Division for publication in the Journal of Heat Transfer. Manuscript received by the Heat Transfer Division April 21, 1986. Keywords: Conduction, Radiation, Radiation Interactions.

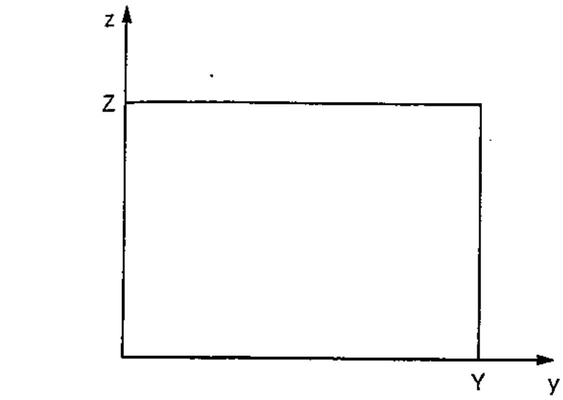

Fig. 1 Geometry and coordinate system for the two-dimensional enclosure

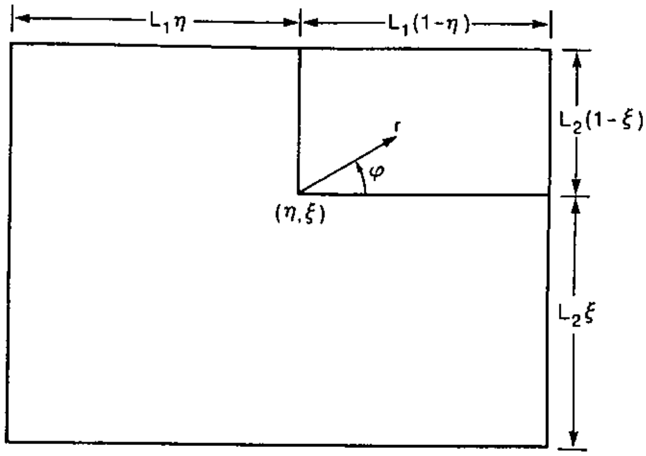

Fig. 2 Domain of integration and the "polar" coordinate used in equation (5)

2 Mathematical Formulation

2(*a*) **Basic Equations.** Consider a rectangular enclosure with an associated coordinate system as shown in Fig. 1. The governing equation for combined conductive-radiative heat transfer is well known. For an enclosure with black walls and a nonscattering medium with constant properties and no internal heat generation, it can be written as

$$\frac{4N_1}{L_1^2}\frac{\partial^2\vartheta}{\partial\eta^2}+\frac{4N_1}{L_2^2}\frac{\partial^2\vartheta}{\partial\zeta^2}+L_1L_2\int_0^1\int_0^1 F(\eta',\zeta')\frac{S_1(d_0)}{d_0}\,d\eta'd\zeta' \tag{1}$$

$$=4F-L_1L_2(1-\vartheta_2^4)\zeta\int_0^1\frac{S_2(d_1)}{d_1^2}\,d\eta'$$

where

$$d_0=[L_1^2(\eta-\eta')^2+L_2^2(\zeta-\zeta')^2]^{1/2} \tag{2a}$$

$$d_1=[L_1^2(\eta-\eta')^2+L_2^2\zeta^2]^{1/2} \tag{2b}$$

$$\vartheta=\frac{T}{T_1},\quad F=\vartheta^4-\vartheta_2^4 \tag{2c}$$

$$N_1=\frac{ka}{4\sigma T_1^3} \tag{2d}$$

$$L_1=aY,\quad L_2=aZ \tag{2e}$$

$$\eta=\frac{y}{Y},\quad \zeta=\frac{z}{Z} \tag{2f}$$

with $\vartheta_2=T_2/T_1$ and T_1 and T_2 being the temperature of the lower wall and the remaining boundary, respectively. N_1 is the familiar conduction-radiation parameter with k and a being the thermal conductivity and absorption coefficient of he medium, respectively. The functions $S_1(x)$ and $S_2(x)$ belong to a class of generalized exponential integral function defined by

$$S_n(x)=\frac{2}{\pi}\int_1^\infty\frac{e^{-xt}dt}{t^n(t^2-1)^{1/2}} \tag{3}$$

This function has been studied extensively and applied successfully to solutions of two-dimensional pure radiation problems in previous works by Yuen et al. (1984a, 1984b, 1985). The boundary conditions for equation (1) are

$$\begin{aligned}\vartheta(\eta,0)&=1.0\\ \vartheta(\eta,1)&=\vartheta_2\\ \vartheta(0,\zeta)&=\vartheta_2\\ \vartheta(1,\zeta)&=\vartheta_2\end{aligned} \tag{4}$$

Nomenclature

- a = absorption coefficient
- $A_{m,n,i,j}$ = coefficient defined by equation (9)
- $B_{i,j}$ = coefficient defined by equation (9)
- d_0 = optical distance, equation (2*a*)
- d_1 = optical distance, equation (2*b*)
- F = dimensionless emissive power, equation (2*c*)
- k = thermal conductivity
- L_1 = optical thickness in the y direction, equation (2*e*)
- L_2 = optical thickness in the z direction, equation (2*e*)
- N_1 = conduction-radiation parameter, equation (2*d*)
- q_a = heat flux calculated by the additive solution, equation (10)
- q_r = heat flux calculated by a pure radiation analysis
- r = radial coordinate, Fig. 2
- S_n = general exponential integral function, equation (3)
- T_1 = temperature of the hot lower wall
- T_2 = temperature of the cold wall
- y = coordinate, Fig. 1
- Y = dimension of the enclosure, Fig. 1
- z = coordinate, Fig. 1
- Z = dimension of the enclosure, Fig. 1
- β_c = dimensionless temperature gradient calculated by a pure conduction analysis
- ζ = dimensionless coordinate in the z direction, equation (2*f*)
- η = dimensionless coordinate in the y direction, equation (2*f*)
- ϑ = dimensionless temperature, equation (2*c*)
- ϑ_2 = T_2/T_1
- σ = Stefan–Boltzmann constant
- φ = angular coordinate, Fig. 2
- φ_1 = angle parameter, equation (6*a*)
- φ_2 = angle parameter, equation (6*b*)

As in previous analyses for two-dimensional pure radiation problems utilized by Yuen et al. (1984a, 1984b, 1985), the integrals appearing in equation (1) are reformulated, for convenience, in terms of a "polar" coordinate as shown in Fig. 2. Equation (1) becomes

$$\frac{4N_1}{L_1^2}\frac{\partial^2\vartheta}{\partial\eta^2}+\frac{4N_1}{L_2^2}\frac{\partial^2\vartheta}{\partial\zeta^2}$$
$$+\iint_{(r,\varphi)}F\left(\eta+\frac{r}{L_1}\cos\varphi,\ \zeta+\frac{r}{L_2}\sin\varphi\right)S_1(r)drd\varphi \tag{5}$$
$$=4F-(1-\vartheta_2^4)\int_{\varphi_1}^{\varphi_2}S_2(L_2\zeta\sec\varphi)d\varphi$$

with

$$\varphi_1=\tan^{-1}\frac{L_1\eta}{L_2\zeta} \tag{6a}$$

$$\varphi_2=\tan^{-1}\frac{L_1(1-\eta)}{L_2\zeta} \tag{6b}$$

2(*b*) Numerical Procedure. Solutions to equation (5) are generated numerically by finite difference. Specifically, the medium is first divided into an $M_1\times M_2$ interior grid such that the coordinate of each interior grid point is given by

$$\eta_i=i\ \delta\eta,\qquad i=1,\ldots,M_1 \tag{7a}$$
$$\delta\eta=\frac{1}{M_1+1}$$
$$\zeta_j=j\ \delta\zeta,\qquad j=1,\ldots,M_2 \tag{7b}$$
$$\delta\zeta=\frac{1}{M_2+1}$$

Equation (5) is then evaluated at the $M_1\times M_2$ grid points to generate a set of M_1M_2 equations for the M_1M_2 unknown temperatures and emissive powers.

Based on a usual Taylor-series expansion of the dimensionless temperature ϑ, the conduction term in equation (5) can be written as

$$\frac{4N_1}{L_1^2}\frac{\partial^2\vartheta}{\partial\eta^2}+\frac{4N_1}{L_2^2}\frac{\partial^2\vartheta}{\partial\zeta^2}$$
$$=\frac{4N_1}{L_1^2}\frac{\vartheta_{i-1,j}+\vartheta_{i+1,j}-2\vartheta_{i,j}}{\delta\eta^2} \tag{8}$$
$$+\frac{4N_1}{L_2^2}\frac{\vartheta_{i,j-1}+\vartheta_{i,j+1}-2\vartheta_{i,j}}{\delta\zeta^2}$$

Utilizing a linearized distribution of F within each rectangular element as in Yuen and Ho (1985), the radiation term becomes

$$\iint_{(r,\varphi)}F(\eta_i+\frac{r}{L_1}\cos\varphi,\ \zeta_j+\frac{r}{L_2}\sin\varphi)S_1(r)drd\varphi$$
$$+(1-\vartheta_2^4)\int_{\varphi_1}^{\varphi_2}S_2(L_2\zeta_j\sec\varphi)d\varphi \tag{9}$$
$$=\sum_{m,n=1}^{m,n=M}A_{i,j,m,n}F_{m,n}+B_{i,j}$$

The coefficients $B_{i,j}$ and $A_{i,j,m,n}$ are identical to those generated in the appendix of the previous work (Yuen and Ho, 1985). They are, in general, functions of geometry only and can be readily evaluated based on tabulated values of $S_n(x)$. A set of coefficients, similar to $A_{i,j,m,n}$, must also be tabulated for the evaluation of radiative heat flux. For a typical calculation ($L_1=L_2=1$, $M_1=M_2=10$), the cpu time required for the evaluation of these coefficients is less than 3 min on a 11/780 Vax computer.

Note that in the development of equation (9), the value of F at the boundary is generated by linear interpolation of its values at the two closest grid points in the direction normal to the boundary. It thus does not satisfy the no-slip temperature boundary condition. Since the function F has, in general, a much steeper gradient near the boundary than the function ϑ, a linear approximation for F that does not satisfy the temperature boundary condition yields a better approximation of the radiative contribution to the energy balance. Numerical experiments show that this greatly increases the accuracy of the result, particularly for cases with relatively large grid sizes.

Numerical solutions to equation (5) are generated by iteration. In contrast to many existing works on combined conductive-radiative heat transfer, the present work utilizes different iteration procedures depending on the value of the conduction-radiation parameter. In the limit of large N_1, the conduction term is expected to have the most significant influence on the temperature distribution. Solutions are generated by a conductive iteration in which, at each step of the iteration, the radiative term is evaluated using the temperature distribution calculated at the previous iteration step and considered as a source term. The new temperature distribution is then determined by a matrix inversion of the conduction term. In the limit of small N_1, on the other hand, the effect of radiation is expected to dominate. The emissive power distribution is determined by a radiative iteration in which the conduction term is evaluated using the emissive power determined by the previous iterative step and considered as a source term. The new emissive power distribution is generated by a matrix inversion of the radiative term. For all cases considered, one or both of the above iteration techniques are effective in generating numerical solutions efficiently. For cases with

Table 1 Maximum value of Δ_φ, Δ_{q_η}, and Δ_{q_ζ} in percent along the horizontal and vertical centerlines between the 11 × 11 and 21 × 21 calculations for a square enclosure with various values of L_1 and N_1

$L_1=L_2$		$N_1=1.0$	0.1	0.01	0.001
0.1	Δ_φ	0.16	0.16	0.14	0.09
	Δ_{q_η}	1.57	1.40	0.64	0.61
	Δ_{q_ζ}	3.88	2.36	0.43	0.33
0.5	Δ_φ	0.15	0.12	0.06	0.42
	Δ_{q_η}	1.47	1.26	1.95	0.82
	Δ_{q_ζ}	3.12	0.76	1.12	0.50
1.0	Δ_φ	0.15	0.09	0.19	0.35
	Δ_{q_η}	1.38	2.05	2.40	1.07
	Δ_{q_ζ}	2.61	1.07	1.53	0.64
2.0	Δ_φ	0.12	0.05	0.12	0.14
	Δ_{q_η}	1.29	2.61	1.95	1.44
	Δ_{q_ζ}	2.17	1.28	1.99	0.89
5.0	Δ_φ	0.11	0.06	0.55	0.53
	Δ_{q_η}	2.88	3.40	4.77	4.90
	Δ_{q_ζ}	2.88	3.40	6.12	3.67

Table 2(a) $\varphi(0.5, \zeta)$ and $q_\zeta(0.5, \zeta)$ for square enclosures with $L_1 = L_2 = 0.1$ and various values of N_1

N_1	ζ = 1.0	0.7	0.5	0.3	0.0
1.0	φ = 0.500	0.560	0.625	0.733	1.000
	q_ζ = 7.473	10.795	17.369	28.074	41.144
0.1	φ = 0.500	0.561	0.626	0.733	1.000
	q_ζ = 1.100	1.542	2.305	3.503	4.932
0.01	φ = 0.500	0.567	0.633	0.738	1.000
	q_ζ = 0.482	0.616	0.798	1.046	1.311
0.001	φ = 0.500	0.615	0.680	0.766	1.000
	q_ζ = 0.398	0.524	0.648	0.801	0.949

Table 2(b) $\varphi(0.5, \zeta)$ and $q_\zeta(0.5, \zeta)$ for square enclosures with $L_1 = L_2 = 1.0$ and various values of N_1

N_1	ζ = 1.0	0.7	0.5	0.3	0.0
1.0	φ = 0.500	0.564	0.630	0.737	1.000
	q_ζ = 0.927	1.352	2.112	3.315	4.701
0.1	φ = 0.500	0.589	0.661	0.763	1.000
	q_ζ = 0.289	0.430	0.609	0.860	1.083
0.01	φ = 0.500	0.653	0.726	0.807	1.000
	q_ζ = 0.222	0.344	0.463	0.610	0.730
0.001	φ = 0.500	0.685	0.736	0.794	1.000
	q_ζ = 0.226	0.322	0.423	0.556	0.722

Table 2(c) $\varphi(0.5, \zeta)$ and $q_\zeta(0.5, \zeta)$ for square enclosures with $L_1 = L_2 = 5.0$ and various values of N_1

N_1	ζ = 1.0	0.7	0.5	0.3	0.0
1.0	φ = 0.500	0.567	0.640	0.755	1.000
	q_ζ = 0.173	0.298	0.514	0.858	1.034
0.1	φ = 0.500	0.585	0.689	0.834	1.000
	q_ζ = 0.039	0.130	0.257	0.408	0.253
0.01	φ = 0.500	0.658	0.732	0.814	1.000
	q_ζ = 0.068	0.111	0.165	0.245	0.388
0.001	φ = 0.500	0.665	0.738	0.817	1.000
	q_ζ = 0.071	0.110	0.161	0.238	0.380

$\vartheta_2 = 0.5$ and $L_1 = L_2 = 1.0$, for example, the conductive iteration is effective in generating solutions with $N_1 \geq 0.02$ while the radiative iteration is effective when $N_1 \leq 0.01$. Using pretabulated values for the coefficients $A_{i,j,m,n}$ and $B_{i,j}$, each iterative calculation requires less than 3 min of cpu time on an 11/780 Vax computer.

Table 2(d) $\varphi(\eta, 0.5)$, $q_\eta(\eta, 0.5)$, and $q_\zeta(\eta, 0.5)$ for square enclosures with $L_1 = L_2 = 0.1$ and various values of N_1

N_1	η = 0.6	0.8	1.0
1.0	φ = 0.620	0.577	0.500
	q_ζ = 16.819	11.800	0.395
	q_η = 4.347	12.619	16.839
0.1	φ = 0.621	0.578	0.500
	q_ζ = 2.241	1.668	0.395
	q_η = 0.494	1.431	1.919
0.01	φ = 0.628	0.583	0.500
	q_ζ = 0.783	0.655	0.395
	q_η = 0.109	0.312	0.427
0.001	φ = 0.674	0.620	0.500
	q_ζ = 0.638	0.554	0.395
	q_η = 0.070	0.200	0.277

Table 2(e) $\varphi(\eta, 0.5)$, $q_\eta(\eta, 0.5)$, and $q_\zeta(\eta, 0.5)$ for square enclosures with $L_1 = L_2 = 1.0$ and various values of N_1

N_1	η = 0.6	0.8	1.0
1.0	φ = 0.624	0.580	0.500
	q_ζ = 2.050	1.489	0.238
	q_η = 0.491	1.422	1.898
0.1	φ = 0.654	0.603	0.500
	q_ζ = 0.595	0.478	0.240
	q_η = 0.107	0.305	0.404
0.01	φ = 0.721	0.669	0.500
	q_ζ = 0.454	0.381	0.245
	q_η = 0.070	0.195	0.250
0.001	φ = 0.733	0.711	0.500
	q_ζ = 0.416	0.357	0.242
	q_η = 0.059	0.171	0.243

3 Results and Discussion

3(*a*) Numerical Accuracy. Numerical results show that except for regions near the two lower corners at which the boundary condition is singular, solutions converge rapidly. To

Table 2(f) $\varphi(\eta, 0.5)$, $q_\eta(\eta, 0.5)$, and $q_\zeta(\eta, 0.5)$ for square enclosures with $L_1 = L_2 = 5.0$ and various values of N_1

N_1	$\eta = 0.6$	0.8	1.0
1.0	$\varphi = 0.634$	0.586	0.500
	$q_\zeta = 0.496$	0.344	0.039
	$q_\eta = 0.125$	0.344	0.418
0.1	$\varphi = 0.681$	0.614	0.500
	$q_\zeta = 0.245$	0.164	0.048
	$q_\eta = 0.059$	0.137	0.113
0.01	$\varphi = 0.728$	0.692	0.500
	$q_\zeta = 0.161$	0.129	0.061
	$q_\eta = 0.034$	0.099	0.149
0.001	$\varphi = 0.734$	0.700	0.500
	$q_\zeta = 0.158$	0.128	0.063
	$q_\eta = 0.032$	0.095	0.153

illustrate the numerical accuracy, predictions of the dimensionless temperature and heat fluxes along the vertical and horizontal centerline, ($\eta = 0.5$, ζ) and (η, $\zeta = 0.5$), for a square enclosure ($L_1 = L_2$) generated by an 11×11 calculation ($\delta\eta = \delta\zeta = 0.1$) are compared with those generated by a 21×21 calculation ($\delta\eta = \delta\zeta = 0.05$). As a quantitative indicator of the accuracy of the calculation, the relative error of a parameter f (which can be either φ, q_η, or q_ζ) is introduced as

$$\Delta_f = \frac{f_{11\times 11} - f_{21\times 21}}{f_{11\times 11}} \qquad (10)$$

The maximum values of Δ_φ, $\Delta_{q\zeta}$, and $\Delta_{q\eta}$ along the two center lines for different optical thicknesses and conduction–radiation parameters are tabulated and presented in Table 1. The dimensionless temperature φ is accurate to within 1 percent for all cases while somewhat higher errors (5 and 6 percent, respectively) are observed for q_η and q_ζ. The accuracy of the solution improves as N_1 decreases. For the pure radiation results, φ, q_η, and q_ζ are all accurate (in the whole enclosure including regions near the two corners) to within 1 percent. Physically, these results indicate that radiative transfer is not very sensitive to the localized temperature distribution. Accurate solution can be generated with a relatively "coarse" 11×11 grid. Because of its relative accuracy, the present numerical data can serve as reference "benchmark" solutions for future development of approximation techniques for multidimensional combined mode heat transfer. They are presented in Tables 2(a–f).

For enclosures with L_2/L_1 less than one, numerical experiments show that results generated by an 11×11 calculation are of the same order of accuracy as those presented in Tables 2(a–f). For cases with L_2/L_1 greater than one, additional grid points in the vertical direction are required because a larger fraction of the enclosed medium is away from the heating surface. In general, results with a relative accuracy of 5 percent can be obtained provided the dimensionless grid size in the direction of smaller optical thickness is taken to be 0.1 or less and the optical distance between grid points in the two direction are equal (i.e., $L_1\delta\eta = L_2\delta\zeta$).

Table 3 Nondimensional heat flux distribution at different walls with $L_1 = L_2 = 1.0$

Nondimensional	Bottom(hot) wall nondimensional heat flux				
position η	$N_1 = 1.0$	$N_1 = 0.1$	$N_1 = 0.01$	$N_1 = 0.001$	$N_1 = 0$
0.1	11.019	1.817	0.888	0.792	0.778
0.3	5.615	1.195	0.758	0.736	0.729
0.5	4.701	1.083	0.730	0.722	0.716
Nondimensional	Side(cold) wall nondimensional heat flux				
position ζ	$N_1 = 1.0$	$N_1 = 0.1$	$N_1 = 0.01$	$N_1 = 0.001$	$N_1 = 0$
0.1	10.250	1.452	0.581	0.494	0.487
0.3	3.918	0.698	0.373	0.345	0.344
0.5	1.898	0.404	0.250	0.243	0.244
0.7	0.917	0.233	0.163	0.168	0.170
0.9	0.308	0.110	0.096	0.108	0.112
Nondimensional	Top(cold) wall nondimensional heat flux				
position η	$N_1 = 1.0$	$N_1 = 0.1$	$N_1 = 0.01$	$N_1 = 0.001$	$N_1 = 0$
0.1	0.373	0.176	0.163	0.175	0.178
0.3	0.778	0.260	0.207	0.213	0.216
0.5	0.927	0.289	0.222	0.226	0.228
	Total nondimensional heat fluxes				
	$N_1 = 1.0$	$N_1 = 0.1$	$N_1 = 0.01$	$N_1 = 0.001$	$N_1 = 0$
Bottom wall	3.157	0.649	0.398	0.379	0.375
Side wall	2.824	0.518	0.289	0.274	0.274
Top wall	0.316	0.114	0.095	0.099	0.101
% error	0.54	2.52	3.54	1.63	0.00

To demonstrate the heat transfer characteristics and to illustrate further the accuracy of the numerical results, heat flux distributions at the bottom, top, and side boundaries, together with the overall energy balance for enclosures with L_1, $L_2 = 1.0$, 0.5, are presented in Tables 3, 4, and 5. It can be readily observed that in all cases overall energy balance is achieved to within 4 percent. In general, the accuracy of the heat flux prediction is equivalent to a similar pure-conduction calculation utilizing an 11×11 grid. Indeed, it is interesting to note that the general overall accuracy of the computation appears to depend on the finite difference approximation of the conduction term. The radiative term, based on the present formulation, is extremely accurate. Additional numerical data for both temperature and heat flux distribution (with L_1, L_2 = 1, 0.5, 1.0, 2.0, 5.0 and $N_1 = 0$, 0.001, 0.01, 0.1, 1.0, 10.0) are presented elsewhere (Takara, 1987).

For a square enclosure with $L_1 = L_2 = 1.0$, the centerline temperature and heat flux distribution presented in Tables 2(a–f) are essentially identical to the graphic results presented by Razzaque et all. (1984). This agreement supports the accuracy of the present calculation. The centerline heat flux generated by the P-3 approximation (Ratzel and Howell, 1982) differs significantly from the present results. This demonstrates the uncertain accuracy of the P-3 approximation.

3(b) Accuracy of the Diffusion Approximation. Because

Table 4 Nondimensional heat flux distribution at different walls with $L_1 = 1.0$ and $L_2 = 0.5$

Nondimensional position η	Bottom(hot) wall nondimensional heat flux $N_1 = 1.0$	$N_1 = 0.1$	$N_1 = 0.01$	$N_1 = 0.001$	$N_1 = 0$
0.1	14.042	2.128	0.934	0.812	0.797
0.3	6.363	1.309	0.807	0.765	0.757
0.5	5.494	1.210	0.786	0.754	0.746
Nondimensional position ζ	**Side(cold) wall nondimensional heat flux $N_1 = 1.0$**	**$N_1 = 0.1$**	**$N_1 = 0.01$**	**$N_1 = 0.001$**	**$N_1 = 0$**
0.1	13.889	1.848	0.653	0.536	0.524
0.3	7.223	1.093	0.484	0.430	0.426
0.5	4.098	0.711	0.373	0.348	0.349
0.7	2.214	0.458	0.285	0.279	0.282
0.9	0.796	0.249	0.202	0.213	0.220
Nondimensional position η	**Top(cold) wall nondimensional heat flux $N_1 = 1.0$**	**$N_1 = 0.1$**	**$N_1 = 0.01$**	**$N_1 = 0.001$**	**$N_1 = 0$**
0.1	1.556	0.461	0.353	0.348	0.349
0.3	3.309	0.743	0.481	0.455	0.453
0.5	3.819	0.827	0.521	0.489	0.486
	Total nondimensional heat fluxes $N_1 = 1.0$	**$N_1 = 0.1$**	**$N_1 = 0.01$**	**$N_1 = 0.001$**	**$N_1 = 0$**
Bottom wall	3.748	0.723	0.420	0.391	0.387
Side wall	2.419	0.396	0.196	0.181	0.181
Top wall	1.319	0.317	0.218	0.207	0.207
% error	0.25	1.28	1.99	1.13	0.10

Table 5 Nondimensional heat flux distribution at different walls with $L_1 = 0.5$ and $L_2 = 1.0$

Nondimensional position η	Bottom(hot) wall nondimensional heat flux $N_1 = 1.0$	$N_1 = 0.1$	$N_1 = 0.01$	$N_1 = 0.001$	$N_1 = 0$
0.1	21.278	2.896	1.000	0.864	0.836
0.3	10.576	1.779	0.898	0.828	0.809
0.5	8.772	1.587	0.871	0.816	0.802
Nondimensional position ζ	**Side(cold) wall nondimensional heat flux $N_1 = 1.0$**	**$N_1 = 0.1$**	**$N_1 = 0.01$**	**$N_1 = 0.001$**	**$N_1 = 0$**
0.1	11.681	1.532	0.520	0.410	0.405
0.3	2.708	0.481	0.253	0.227	0.228
0.5	0.824	0.200	0.134	0.128	0.130
0.7	0.268	0.093	0.073	0.075	0.077
0.9	0.077	0.040	0.038	0.042	0.045
Nondimensional position η	**Top(cold) wall nondimensional heat flux $N_1 = 1.0$**	**$N_1 = 0.1$**	**$N_1 = 0.01$**	**$N_1 = 0.001$**	**$N_1 = 0$**
0.1	0.098	0.082	0.083	0.092	0.097
0.3	0.143	0.098	0.094	0.101	0.105
0.5	0.159	0.103	0.098	0.104	0.108
	Total nondimensional heat fluxes $N_1 = 1.0$	**$N_1 = 0.1$**	**$N_1 = 0.01$**	**$N_1 = 0.001$**	**$N_1 = 0$**
Bottom wall	2.983	0.483	0.230	0.210	0.205
Side wall	2.946	0.455	0.199	0.180	0.180
Top wall	0.032	0.023	0.023	0.024	0.026
% error	0.58	0.57	3.71	2.86	0.03

of the mathematical complexity of radiation, the diffusion approximation (Deisler, 1964) is still a common approximation procedure utilized by most practicing engineers in assessing the importance of radiation in actual multidimensional engineering systems. It is interesting to note, however, that, except for one-dimensional planar systems, the relative accuracy of the diffusion approximation has never been demonstrated quantitatively. The present numerical results are now used to assess the accuracy of the diffusion approximation for two-dimensional combined conduction-radiation problems.

Using an 11×11 grid, numerical results are generated for the same set of values for L_1, L_2, and N_1 based on the diffusion approximation. A complete set of numerical data is presented elsewhere (Takara, 1987). Using an expression similar to equation (10) (with $f_{21 \times 21}$ replaced by f_{dif}), the minimum and maximum values of Δ_φ, Δ_{q_η} and Δ_{q_ζ} for various square enclosures are presented in Table 6. Since the diffusion approximation always predicts a correct φ at the boundary, the minimum Δ_φ is calculated only for the interior points along the two centerlines. It is apparent that while the diffusion approximation is moderately successful in predicting the interior temperature distributions φ (less than 17 percent maximum relative error), it is uniformly inaccurate in predicting heat transfer. The validity of many existing practical engineering calculations utilizing the diffusion approximation for the radiative heat transfer effect is thus highly uncertain.

3(c) Accuracy of the Additive Solution. In one-dimensional combined conductive–radiative heat transfer

Table 6 Maximum (minimum) value of Δ_φ, Δ_{q_η}, and Δ_{q_ζ} in percent along the horizontal and vertical centerlines between the numerical results and the diffusion approximation and an 11×11 grid for a square enclosure with various values of L_1 and N_1

$L_1 = L_2$		$N_1 = 1.0$	0.1	0.01	0.001
0.1	Δ_φ	6.20(1.29)	15.02(5.06)	16.30(5.38)	9.67(2.13)
	Δ_{q_η}	60.01(59.98)	57.43(56.56)	531.69(516.30)	871.27(836.27)
	Δ_{q_ζ}	100.00(60.27)	100.00(3.60)	387.37(86.98)	563.32(100.00)
0.5	Δ_φ	5.98(1.18)	12.60(4.03)	7.11(0.27)	10.19(0.01)
	Δ_{q_η}	62.31(62.22)	3.32(1.97)	85.48(81.68)	111.24(102.78)
	Δ_{q_ζ}	100.00(63.04)	100.00(9.01)	100.00(5.68)	100.00(0.25)
1.0	Δ_φ	5.52(1.00)	9.23(2.72)	4.81(0.04)	10.06(0.21)
	Δ_{q_η}	64.60(64.49)	27.66(27.61)	5.36(0.97)	14.08(6.79)
	Δ_{q_ζ}	100.00(65.23)	100.00(32.66)	100.00(12.51)	100.00(12.47)
2.0	Δ_φ	4.62(0.83)	5.64(2.08)	7.34(0.64)	10.14(0.18)
	Δ_{q_η}	67.93(87.01)	53.37(44.72)	38.90(38.50)	39.84(32.88)
	Δ_{q_ζ}	100.00(67.42)	100.00(47.68)	100.00(46.48)	100.00(44.37)
5.0	Δ_φ	3.25(0.94)	7.19(0.64)	6.55(0.26)	8.15(0.08)
	Δ_{q_η}	72.11(67.78)	73.77(46.96)	64.70(59.64)	68.12(58.51)
	Δ_{q_ζ}	100.00(68.78)	100.00(34.27)	100.00(63.64)	100.00(62.98)

Table 7 Maximum (minimum) value of Δ_φ, Δ_{q_η}, and Δ_{q_ζ} in percent along the horizontal and vertical centerlines between the numerical results and the additive solution with an 11 × 11 grid for a square enclosure with various values of L_1 and N_1

$L_1 = L_2$		$N_1 = 1.0$	0.1	0.01	0.001
0.1	Δ_{q_η}	0.02(0.01)	0.20(0.10)	0.87(0.42)	1.24(0.40)
	Δ_{q_ζ}	0.48(0.00)	0.48(0.00)	0.64(0.01)	0.69(0.09)
0.5	Δ_{q_η}	0.33(0.08)	2.11(0.42)	4.95(0.35)	1.77(1.06)
	Δ_{q_ζ}	0.73(0.03)	1.75(0.02)	2.79(0.77)	1.08(0.38)
1.0	Δ_{q_η}	1.04(0.20)	5.78(1.39)	10.60(4.32)	1.11(0.85)
	Δ_{q_ζ}	1.38(0.27)	4.30(0.46)	6.22(0.19)	1.19(0.08)
2.0	Δ_{q_η}	2.73(0.47)	14.66(3.37)	4.41(3.54)	0.88(0.50)
	Δ_{q_ζ}	10.26(0.50)	19.31(0.95)	5.82(0.05)	1.07(0.00)
5.0	Δ_{q_η}	16.12(0.38)	85.04(7.58)	5.50(2.02)	0.85(0.16)
	Δ_{q_ζ}	60.46(0.71)	119.18(0.23)	7.05(0.06)	0.99(0.00)

analysis, it is well know that the additive solution generated by separate independent analyses of the two transfer processes is an accurate approximation (within 10 percent) to the total heat transfer (Einstein, 1963; Yuen and Wong, 1980). For the present two-dimensional problem, an additive solution for the heat transfer can be written as

$$q_a = 4N_1\beta_c + q_r \tag{11}$$

where β_c is the appropriate temperature gradient calculated from a pure conduction analysis and q_r is the radiative flux generated by a pure radiation analysis of the same enclosure. Utilizing numerical results generated from an 11×11 pure conduction analysis ($\delta\eta = \delta\zeta = 0.1$) and results of a pure radiation analysis presented in a previous work (Yuen and Wong, 1984), the maximum and minimum values of Δ_{q_η} and Δ_{q_ζ} for various square enclosures are tabulated and presented in Table 7. The additive approximation appears to be a reasonable estimate for both components of the heat flux over the whole enclosure. Physically, this result suggests that for the estimate of heat transfer, the interaction between conduction and radiation can be considered as sufficiently weak that each process acts almost independently. It is important to note, however, that the additive solution cannot be used to predict the temperature profile.

4 Conclusions

Results of a two-dimensional combined conductive-radiative heat transfer analysis are presented. Based on a numerical technique developed previously for a two-dimensional analysis of radiative transfer and an iteration procedure utilized for a previous one-dimensional combined conductive-radiative analysis, numerical results are generated accurately and efficiently. Numerical data for temperature and heat flux distributions are presented.

Based on numerical results, the accuracy of two commonly used approximation methods for radiative transfer is assessed. The diffusion approximation is shown to be uniformly inaccurate for two-dimensional combined conduction radiation problems. For all optical thicknesses and conduction-radiation parameters considered (including the optically thick limit), the diffusion approximation is shown to yield significant errors in both the temperature and heat flux predictions. The additive solution, on the other hand, appears to be an effective empirical approach in estimating heat transfer. The success of the additive solution suggests that in multidimensional combined conduction-radiation problems, the interaction between radiation and conduction can be considered as sufficiently weak that the two processes contribute independently to the total heat transfer.

References

Deisler, R. G., 1964, "Diffusion Approximation for Thermal Radiation in Gases With Jump Boundary Condition," ASME JOURNAL OF HEAT TRANSFER, Vol. 86, No. 2, pp. 240-246.

Einstein, T. H., 1963, "Radiant Heat Transfer to Absorbing Gases Enclosed Between Parallel Flat Plates With Flow and Conduction," NASA TR R-154.

Glatt, L., and Olfe, D. B., 1973, "Radiative Equilibrium of a Gray Medium in a Rectangular Enclosure," *Journal of Quantitative Spectroscopy and Radiative Transfer*, Vol. 13, p. 881.

Larsen, M. E., and Howell, J. R., 1985, "The Exchange Factor Method: An Alternative Basis for Zonal Analysis of Radiating Enclosure," ASME JOURNAL OF HEAT TRANSFER, Vol. 107, No. 4, pp. 936-942.

Modest, M. F., 1975, "Radiative Equilibrium of a Gray Medium in a Rectangular Enclosure Bounded by Gray Walls," *Journal of Quantitative Spectroscopy and Radiative Transfer*, Vol. 15, p. 445.

Ratzel, A. C., and Howell, J. R., 1982, "Two-Dimensional Radiation in Absorbing-Emitting-Scattering Media Using the P-N Approximation," ASME Paper No. 82-HT-19.

Ratzel, A. C., and Howell, J. R., 1982, "Two-Dimensional Energy Transfer in Radiatively Participating Media With Conduction by the P-N Approximation," *Proceedings of the Seventh International Heat Transfer Conference*, Vol. R14, pp. 535-540.

Razzaque, M. M., Howell, J. R., and Klein, D. E., 1984, "Coupled Radiative and Conductive Heat Transfer in a Two-Dimensional Rectangular Enclosure With Gray Participating Media Using Finite Elements," ASME JOURNAL OF HEAT TRANSFER, Vol. 106, pp. 613-619.

Takara, E., 1987, "Two-Dimensional Combined Conductive Radiative Heat Transfer," M. S. Thesis, University of California, Santa Barbara, in preparation.

Viskanta, R., and Grosh, R. J., 1962, "Heat Transfer by Simultaneous Conduction and Radiation in an Absorbing Medium," ASME JOURNAL OF HEAT TRANSFER, Vol. 84, pp. 63-72.

Yuen, W. W., and Wong, L. W., 1980, "Heat Transfer by Conduction and Radiation in a One-Dimensional Abosrbing, Emitting and Anisotropically Scattering Medium," ASME JOURNAL OF HEAT TRANSFER, Vol. 102, pp. 303-307.

Yuen, W. W., and Wong, L. W., 1984, "Analysis of Radiative Equilibrium in a Rectangular Enclosure With Gray Medium," ASME JOURNAL OF HEAT TRANSFER, Vol. 106, pp. 433-440.

Yuen, W. W., 1984, "Analysis of Radiative Equilibrium in a Rectangular Enclosure With Gray Medium: Cases With Diffusely Reflecting Surfaces and Heat Flux Boundary Conditions," presented at the 1984 ASME Winter Annual Meeting, New Orleans, LA, Dec.

Yuen, W. W., and Ho, C. F., 1985, "Analysis of Two-Dimensional Radiative Heat Transfer in a Gray Medium With Internal Heat Generation," *International Journal of Heat and Mass Transfer*, Vol. 28, No. 1, pp. 17-23.